Biochemistry

 Volume 36, Number 42 October 21, 1997

Accelerated Publications

Calicheamicin-Mediated DNA Damage in a Reconstituted Nucleosome Is Not Affected by Histone Acetylation: The Role of Drug Structure in the Target Recognition Process†

Qi Liang, Deok-Joon Choi, and Peter C. Dedon*

Division of Toxicology, 56-787, Massachusetts Institute of Technology, Cambridge, Massachusetts 02139

Received July 29, 1997; Revised Manuscript Received September 3, 1997⊗

ABSTRACT: We have examined the role of drug structure and histone acetylation in DNA damage produced by the enediyne antibiotic calicheamicin γ_1^I in nucleosomes reconstituted onto the 5S rRNA gene of *Xenopus borealis*. Consistent with previous observations, calicheamicin damage at the 3′-end of a purine tract (positions −13 and −14) was enhanced in the nucleosome compared to naked DNA while damage at other sites was somewhat reduced in the nucleosome. However, damage produced by esperamicin C, an analog of calicheamicin missing the terminal sugar-aromatic ring in the side chain, showed no enhancement at positions −13 and −14, and its sequence selectivity in naked DNA was markedly different from that of calicheamicin. This highlights the importance of the intact tetrasaccharide side chain in the recognition of the structural deformation occurring at the 3′-ends of purine tracts. Both drugs produced identical cleavage patterns in normal and hyperacetylated nucleosomes. Given the sensitivity of calicheamicin to local DNA conformation, this observation is consistent with other studies that suggest that histone acetylation alone does not significantly affect the local conformation of core DNA in the nucleosome.

Considerable attention has been focused on understanding the relationship between drug structure and the selection of DNA targets *in vitro* (e.g., ref 1). However, the structural perturbations associated with the incorporation of DNA into chromatin add another dimension to the complexity of target recognition by small molecules. This is illustrated by previous studies of DNA damage produced by the enediyne antitumor antibiotics in chromatin and reconstituted nucleosomes (*2*−*4*). It was observed that calicheamicin γ_1^I is capable of damaging the constrained core DNA of the nucleosome (*2*−*4*) and that the damage was enhanced at one site in a nucleosome reconstituted onto a fragment of the 5S rRNA gene of *X. borealis* (*2*, *4*). Given the variation in nucleosome structure that occurs in different states of transcriptional activity, we have now investigated the effect of histone acetylation on the selection of nucleosomal targets by calicheamicin. We have also examined the role of the tetrasaccharide side chain of calicheamicin in the target recognition process.

The enediyne family of antitumor antibiotics presents a unique opportunity to study the relationship between drug structure and DNA conformation that is involved in the recognition of DNA targets. Like other enediynes, calicheamicin is an extremely potent cytotoxin that binds in the minor groove of DNA and, following thiol activation, forms a diradical intermediate that abstracts hydrogen atoms from deoxyribose on each strand (reviewed in

† Supported by NIH/NCI grant CA64524 (P.C.D.) and the Samuel A. Goldblith Professorship (P.C.D.).

* Author to whom correspondence should be addressed. Tel: (617) 253-8017. Fax: (617) 258-0225. E-mail: pcdedon@mit.edu.

⊗ Abstract published in *Advance ACS Abstracts,* October 1, 1997.

S0006-2960(97)01839-4 CCC: $14.00

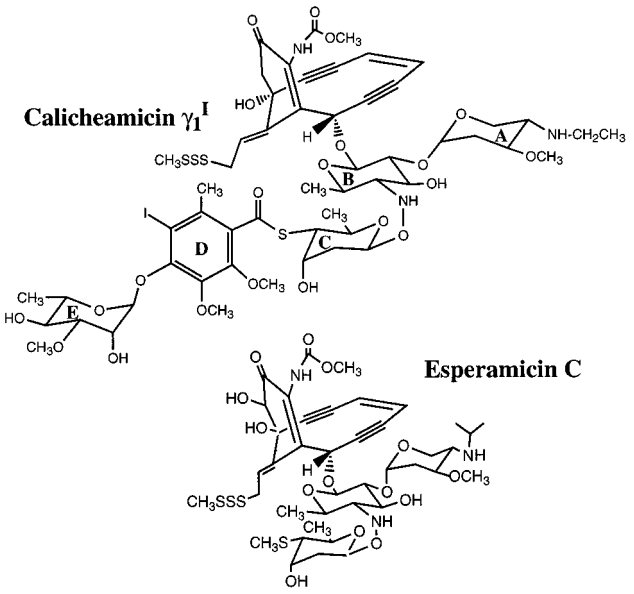

FIGURE 1: Structures of calicheamicin γ_1^I and esperamicin C.

refs 5 and 6). The resulting damage consists almost entirely of bistranded lesions produced by a single drug molecule (*7*).

While this chemistry has been firmly established, the mechanism by which enediynes select their DNA targets is not well understood. Calicheamicin is unusual among small molecules for its DNA sequence selectivity, which was initially associated with tetrapurine sequences such as AGGA, AAAA, and GAGA (*8*−*10*). However, more recent studies have revealed that the drug generally targets the 3′-ends of purine tracts, both runs of adenine, and mixed A/G sequences (*4*, *11*). Calicheamicin binds in the minor groove with its aglycone positioned 3′ to the purine tract and with its carbohydrate tail directed toward the 5′-end of the purine tract (*12*−*16*). The major element of target selection has been ascribed to the aryltetrasaccharide (*14*, *17*, *18*). While the aglycone cleaves DNA without apparent sequence selectivity (*18*), the aryltetrasaccharide binds to DNA in roughly the same location as the parent drug (*17*, *19*). Progressive removal of the components of the tetrasaccharide reduces the sequence selectivity of calicheamicin. Esperamicin C, an analog of calicheamicin missing the D and E rings of the carbohydrate tail (Figure 1), has a broad sequence selectivity similar to esperamicin A1 (e.g., TG, CG, tripyrimidine sequences; *20*), while further removal of ring C results in a sequence nonselective pattern of damage similar to the aglycone (*9*).

Recently, it has been established that DNA conformation and dynamics play a critical role in target recognition by calicheamicin. Calicheamicin binding appears to cause bending of the DNA (*21*) possibly as a result of a hinge-like flexibility or other structural perturbation associated with the 3′-ends of purine tracts. It is possible that this bending occurs toward a compressed major groove given the NMR studies that indicate widening of the minor groove around the aglycone (*12*, *13*, *16*). Additionally, calicheamicin binding produces changes in circular dichroism consistent with DNA overwinding, and it induces negative writhing of plasmid DNA (LaMarr *et al.*, submitted for publication; *22*).

These features of calicheamicin targets in naked DNA are analogous to the conformation of DNA in nucleosomes. One of the basic elements of chromatin structure, the nucleosome consists of essentially two regions, core and linker (*23*, *24*). The core is composed of ∼146 base pairs (bp) of DNA wrapped ∼1.8 times in a left-handed superhelix around four pairs of histone proteins, and the linker represents the 20−60 bp of DNA joining adjacent cores. In addition to the bending-induced changes in minor groove width, there are several features of core DNA structure pertinent to target recognition by calicheamicin. These include (1) both helical underwinding (*25*) and an S-shaped bend in the ∼30 bp of core DNA surrounding the dyad axis (*26*); (2) helical overwinding of the remaining ∼120 bp of core DNA (*25*); and (3) sharp bending of the core DNA at four sites symmetrically positioned at one and four helical turns from the dyad axis (*26*, *27*).

Recent studies in nucleosomes reconstituted onto a fragment of the 5S rRNA gene of *X. borealis* suggest that calicheamicin recognizes features of DNA conformation associated with nucleosomes. We and others observed that, while calicheamicin-induced damage was generally reduced in the core DNA, damage was enhanced severalfold at the 3′-end of a purine tract positioned approximately one helical turn away from the dyad axis (*2*, *4*). This enhancement of DNA damage may reflect the formation of a more favorable binding site by bending of the DNA in the nucleosome.

The reconstituted nucleosome used in the previous studies is a model for a canonical nucleosome associated with transcriptionally silent DNA. However, there are several variations in nucleosome structure associated with transcriptionally active genes, one of which involves acetylation of lysine residues in the N-terminal tails of core histone proteins (reviewed in refs 28 and 29). Neutralization of the positive charge of lysine by acetylation appears to alter several features of nucleosome structure. While the question of unwinding of the ends of the core DNA remains controversial (*30*, *31*), acetylation increases the accessibility of the DNA to binding of transcription factors (*32*), reduces the linking number change associated with incorporation of DNA into a nucleosome (*33*), and increases the electrophoretic mobility (*34*) and sedimentation of nucleosomes (*35*). Thermal denaturation and DNase I digestion studies suggest that acetylation relaxes protein−DNA contacts throughout the nucleosome, with an increased overall susceptibility to DNase I cleavage that is most marked ∼60 bp from the ends of the core DNA (*35*). This DNase I sensitive site is located near the calicheamicin target that experiences more damage when the DNA is incorporated into a nucleosome (*4*). In spite of the altered DNase I cleavage, Bauer *et al.* observed no change in the hydroxyl radical cleavage of DNA in acetylated nucleosomes (*30*).

To help resolve these issues, we have examined the effect of histone acetylation on calicheamicin target selection in nucleosomes. In addition, we have attempted to define the role of the tetrasaccharide side chain in the recognition of nucleosomal DNA targets.

EXPERIMENTAL PROCEDURES

Materials. Calicheamicin γ_1^I was generously provided by Dr. George Ellestad (Wyeth-Ayerst Research). Esperamicin C was prepared by acid-catalyzed methanolysis of esperamicin A1 as described elsewhere (*36*). The plasmid pXP-10,

containing the 5S rRNA gene of *X. borealis*, was kindly provided by Dr. Alan Wolffe [NIH/NICHHD; (*37*)].

Purification of Normal and Hyperacetylated Histones. Hyperacetylation of histone proteins was achieved by growing HeLa S3 cells (American Type Culture Collection) to a density of $\sim 4 \times 10^5$/mL in Joklik-modified minimal essential medium (Sigma) supplemented with 10% newborn bovine serum and bringing the culture to 10 mM sodium butyrate 24 h prior to nucleus isolation (*38*, *39*). Nuclei were isolated as described elsewhere (*3*) except that all solutions contained 10 mM sodium butyrate to inhibit histone deacetylase activity (*38*, *39*). Following centrifugation at 2500*g*, the nuclear pellet was rinsed twice with 1 mM HEPES, 0.1 mM EDTA, and 10 mM sodium butyrate (or 10 mM NaCl for normal chromatin), pH 7. The nuclei were then subjected to three 10 s bursts of sonication in the same buffer at a DNA concentration of 0.4 mg/mL with a Branson Model 250 Sonifier equipped with a microprobe and at the lowest setting. The suspension was subjected to centrifugation at 9000*g* for 3 min and the resulting supernatant saved for histone isolation. Following DNA quantitation by absorbance at 260 nm, core histone proteins were isolated by hydroxylapatite chromatography essentially as described by Simon and Felsenfeld (*40*) except that a batch preparation was performed rather than column chromatography (0.34 mg of DNA/mL Bio-Gel HTP; Bio-Rad). The purified core histone proteins eluted in 2 M NaCl, 50 mM sodium phosphate (pH 7), 1 mM EDTA, and 10 mM sodium butyrate (or 10 mM NaCl) were exhaustively dialyzed against 10 mM HEPES and 1 mM EDTA, pH 7. To concentrate the histone proteins, the samples were lyophilized and redialyzed against the same buffer. Histone protein was quantified by absorbance at 230 nm (*40*) and by reference to histone standards on 15% SDS polyacrylamide gels. The level of acetylation of the histones was characterized by electrophoresis on a 15% polyacrylamide gel (37.5:1 acrylamide:bisacrylamide) containing 6.3 M urea and 5% acetic acid. The wells were loaded with 6.3 M urea, 5% acetic acid, and 0.5 M cysteamine, and the gel was prerun in 5% acetic acid for 3 h. Following lyophilization to dryness, the histones were redissolved in 5 μL of 4 M urea, 5% acetic acid, 0.02% pyronin Y, and 5% 2-mercaptoethanol, heated at 90 °C for 2 min, cooled, and loaded onto the gel. When the pyronin Y had migrated to the bottom of the gel, the gel was fixed and stained with Coomassie Blue, destained, and dried.

Reconstitution of Nucleosomes on 5S rDNA. The 215 bp *Eco*RI/*Dde*I fragment of pXP-10 was 5′-end labeled with [^{32}P] at the *Eco*RI site as described previously (*4*). Nucleosomes were reconstituted from the labeled DNA and purified histones by dialysis from high salt-urea essentially as described elsewhere (*4*), except that sonicated calf thymus DNA ($\sim$500 bp average) was used as cold carrier and the ratio of histone to DNA was 1:1. The degree of incorporation of the DNA into nucleosomes ranged from 75 to 95% (data not shown).

DNA Damage Reactions and Hydroxyl Radical Footprinting. Drug reactions were performed by adding a 1 μL aliquot of a methanolic solution of the drug to naked or nucleosomal DNA (30 μg/mL) in a total of 20 μL reaction volume containing 10 mM glutathione, 15 mM HEPES, and 1 mM EDTA, pH 7; final drug concentrations were 160 nM for calicheamicin and 1.5 μM for esperamicin C. After incubation at 37 °C for 30 min, nucleosomal DNA was resolved from unincorporated DNA on a 4.5% polyacrylamide nucleoprotein gel prepared as described elsewhere (*41*), except that the drug-treated samples were loaded onto the gel following addition of glycerol to a final concentration of 10%. The drug-damaged nucleosome remains intact during this purification due to the low level of DNA damage [data not shown (*2*)]. Hydroxyl radical footprinting studies were performed on naked and nucleosomal DNA as described elsewhere (42), and the damaged nucleosomes were also resolved on a nucleoprotein gel. In all cases, nucleosomes were eluted from the gel by overnight agitation in 300 mM sodium acetate and 1 mM EDTA, pH 7, at 4 °C, and the DNA was purified by phenol/chloroform extraction and ethanol precipitation. The purified DNA was then resolved on an 8% sequencing gel along with Maxam−Gilbert sequencing standards (*43*). Dried gels were subjected to phosphorimager analysis as described elsewhere (*4*). To compensate for lane-to-lane variation in sample loading, radioactivity in each band was expressed as a percentage of the total radioactivity in the lane.

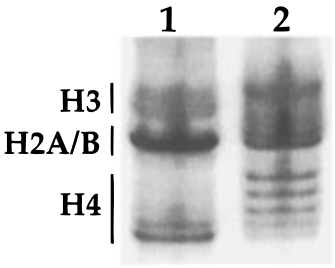

FIGURE 2: Characterization of acetylation levels in preparations of HeLa cell histones. Purified histones from normal (lane 1) and butyrate-treated (lane 2) HeLa cells were resolved on an acid-urea gel as described in Experimental Procedures. The identity of the core histones is noted in the margin.

RESULTS

Characterization of the Reconstituted Nucleosomes. The level of acetylation of histones isolated from control and butyrate-treated HeLa cells is shown in the acid-urea gel in Figure 2. Core histones from butyrate-treated cells are highly acetylated as illustrated most clearly by the multiple bands representing histone H4.

The nucleosomes reconstituted from normal and hyperacetylated histones were characterized by hydroxyl radical footprinting as shown in the gel in Figure 3 and in the line graph in Figure 4A. In both cases, the DNA has the same rotational and translational setting on the histone core as indicated by the identical hydroxyl radical cleavage profiles (Figure 3). The sinusoidal variation in cleavage frequency is due to positioning of the DNA on the histone core, with maxima and minima occurring where the minor groove faces away from and toward the histone core, respectively (*25*).

Calicheamicin Damage in Naked and Nucleosomal 5S rDNA. The damage produced by calicheamicin in naked DNA and in nucleosomes containing normal and hyperacetylated histones is shown in the gel in Figure 3 and in the line graphs in Figure 4 (panels B and C). To ensure that the cleavage patterns apparent in the sequencing gels reflected the true frequency of damage at each site, the studies were performed with a calicheamicin concentration (0.16 μM) that produced on average one or fewer damage

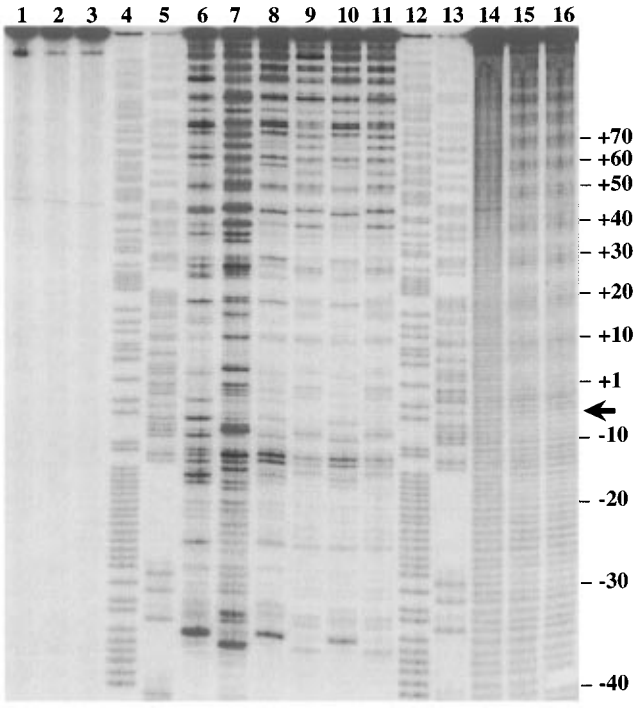

FIGURE 3: Comparison of DNA damage produced by calicheamicin (160 nM) and esperamicin C (1.5 μM) in normal and hyperacetylated nucleosomes. Lanes 1, 6, 7, and 14: naked DNA. Lanes 2, 8, 9, and 15: normal nucleosomes. Lanes 3, 10, 11, and 16: hyperacetylated nucleosomes. Lanes 1−3, untreated controls. Lanes 6, 8, and 10: calicheamicin. Lanes 7, 9, and 11: esperamicin C. Lanes 14−16: Fe-EDTA. Maxam-Gilbert sequencing standards: A+G, lanes 4, 12; C+T, lanes 5, 13. Position in the 5S rDNA construct is denoted in the left margin relative to the transcription start site (+1); the likely location of the dyad axis is denoted by the arrow (*25*).

events per DNA fragment. The fact that there was no increase in the level of unincorporated DNA in drug-treated samples indicates that the damaged nucleosomes remained intact on the nucleoprotein gel (data not shown).

As shown in Figures 3 and 4, the damage produced by calicheamicin in the naked DNA and in "normal" nucleosomes, reconstituted from purified histones, is virtually identical to that observed previously by Yu *et al*. using a 5S rDNA nucleosome reconstituted by histone exchange from core particles (*4*). This attests to the similar nucleosome structures produced by the two different reconstitution methods. In general, calicheamicin produced damage only at sites where the minor groove faced away from the nucleosome core; these sites are indicated by maxima in the hydroxyl radical cleavage patterns (Figure 4A). As observed previously, calicheamicin-induced damage is increased 3 to 4-fold at one site approximately one helical turn away from the putative dyad axis of the nucleosome (positions −13 and −14 in Figure 4).

It is also apparent that histone acetylation does not affect the identity of calicheamicin target sites or the frequency of cleavage at any site, as suggested by the identical cleavage profiles in normal and hyperacetylated nucleosomes in Figure 4C. This lack of an acetylation effect cannot be ascribed to the reconstitution technique or to the quality of nucleosomes. The results of the present studies of calicheamicin-induced damage in 5S rDNA nucleosomes are identical to those observed earlier in which a different reconstitution technique was employed (*4*). The location and frequency of calicheamicin-induced damage are identical in both naked DNA and nucleosomes with low levels of acetylation (*2*, *4*). This confirms the constancy of nucleosome structure for the two different reconstitution procedures.

Damage Produced by Esperamicin C in Naked and Nucleosomal 5S rDNA. To investigate the role of the tetrasaccharide side chain of calicheamicin in the recognition of nucleosomal DNA targets, we examined the damage produced by esperamicin C in naked and nucleosomal DNA. As shown in the gel in Figure 3 and in the line graphs in Figure 5B, esperamicin C behaves in a manner similar to calicheamicin with damage generally reduced in the nucleosome compared to the naked DNA and with damage sites abolished when the minor groove faces the histone proteins. Again, there is no effect of histone acetylation on the esperamicin C damage patterns (Figure 5C). However, there is no obvious similarity of the sequence selectivities of esperamicin C and calicheamicin and, unlike calicheamicin, there is no increase in damage at positions −13 and −14 (Figure 5B).

DISCUSSION

Calicheamicin is a DNA-damaging enediyne antibiotic that recognizes the 3′-ends of purine tracts in naked DNA (*4*, *11*). Our previous studies revealed that, when a calicheamicin recognition sequence is incorporated into a nucleosome, the associated changes in DNA conformation and dynamics can create high-affinity binding sites for the drug (*2*, *4*). We have now systematically extended this observation in two ways. First, we have examined the effect of a biologically important modification of nucleosome structure, histone acetylation, on the recognition of nucleosomal targets by calicheamicin. Second, we have defined the role of drug structure in this target recognition process.

Histone Acetylation Does Not Affect Enediyne Target Recognition in Nucleosomes. Although the basis for target selection by calicheamicin has not been fully defined, it has been established that the drug is sensitive to changes in DNA conformation. For instance, the extent of DNA damage at a particular site is influenced by flanking sequences (*8*, *44*, *45*), while incorporation of DNA into a nucleosome causes both increases and decreases in DNA damage even when the minor groove is fully accessible to the drug (*4*). In light of the present results, the sensitivity of enediynes to DNA conformation suggests that, at least at sites of drug-induced DNA damage, histone acetylation alone does not significantly alter the local conformation of core DNA in the nucleosome. This conclusion is supported by the virtually identical cleavage profiles in normal and hyperacetylated nucleosomes for both esperamicin C and calicheamicin (Figures 4C and 5C). Our results also suggest that histone acetylation does not affect the rotational or translational setting of DNA on the histone core. In addition to superimposible hydroxyl radical cleavage profiles, DNA damage produced by esperamicin C and calicheamicin is inhibited to the same extent in normal and hyperacetylated nucleosomes when the minor groove of a binding site faces the histone proteins, as shown in Figures 4B and 5B. These conclusions are tempered, however, by the possibility that the calicheamicin and esperamicin C may not be sensitive to certain changes in DNA conformation or to changes that occur outside damage sites.

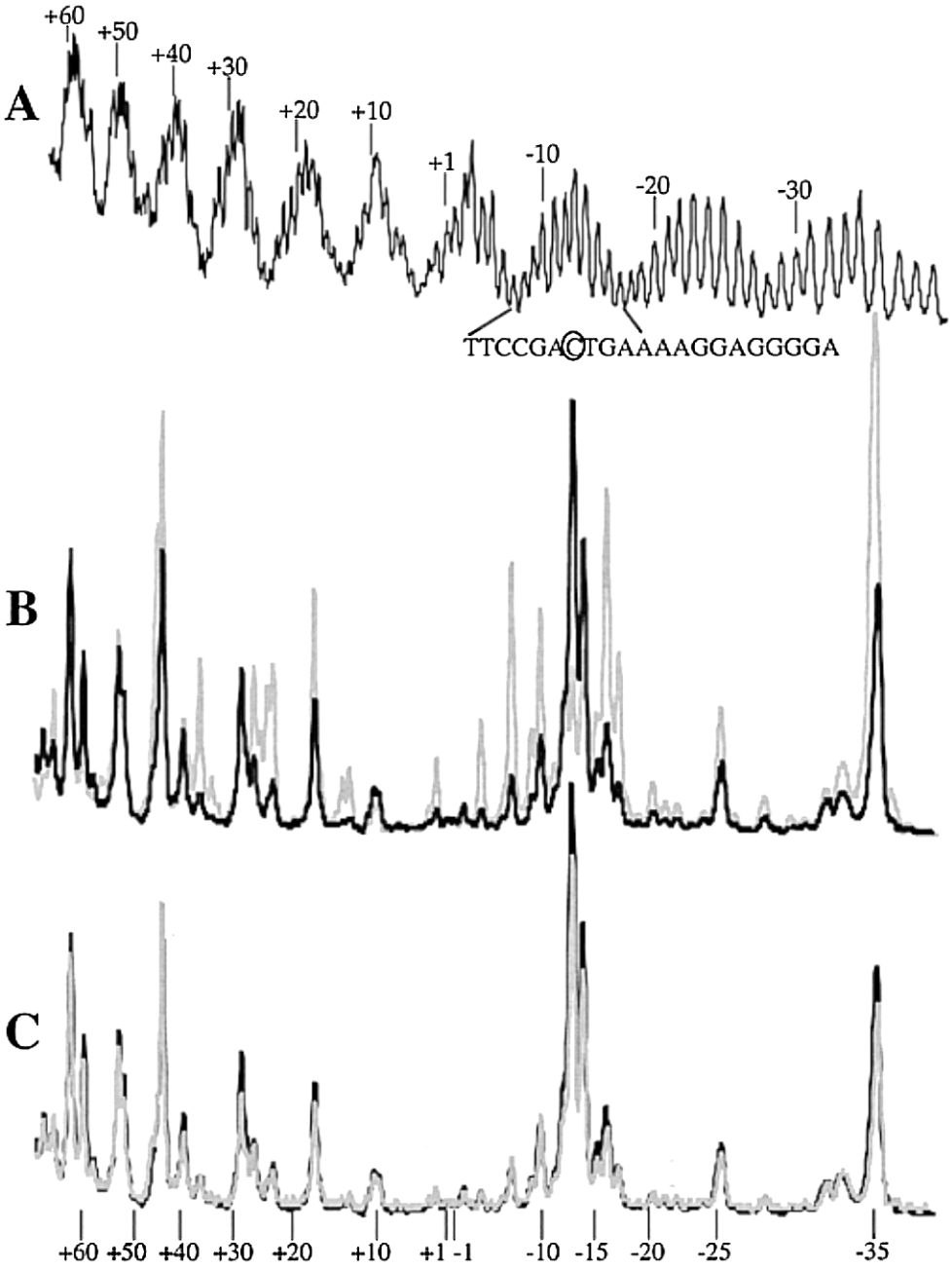

FIGURE 4: Cleavage profiles for calicheamicin and hydroxyl radical in normal and hyperacetylated nucleosomes. The gel shown in Figure 3 was subjected to phosphorimager analysis presented here as line graphs of damage frequency along the 5S rDNA sequence. (A) Hydroxyl radical cleavage of hyperacetylated nucleosomes; the pattern is identical to that produced in normal nucleosomes (data not shown). (B) Overlay of the damage patterns produced by calicheamicin in naked DNA (gray) and normal nucleosomes (black). (C) Overlay of the damage patterns produced by calicheamicin in normal (black) and hyperacetylated nucleosomes (gray). The sequence reads 5′ to 3′ from right to left, with numbering according to the position in the 5S rDNA construct.

Our observations are consistent with the hydroxyl radical cleavage studies of Bauer *et al.* (*30*). They proposed that histone acetylation alters the shape of the nucleosome and thus the number of times the DNA wraps around the histone core, which explains the linking number change that occurs in acetylated nucleosomes (*33*). However, the results of the present studies with enediynes and the hydroxyl radical cleavage studies of Bauer *et al*. (*30*) indicate that this shape change does not significantly affect local DNA conformation in the nucleosome. It is still not clear how these results relate to the increase in DNase I sensitivity of the core DNA in hyperacetylated nucleosomes observed by Ausio and van Holde (*35*). One possible explanation for this observation is that histone acetylation affects the stability of the histone−DNA contacts, as suggested by thermal denaturation studies (*35*). Reduced protein−DNA contacts caused by hyperacetylation of histones may permit relatively large changes in DNA conformation upon binding of DNase I (MW = ∼31 000), while small perturbations induced by the enediynes (calicheamicin MW = 1367) may be tolerated in both normal and hyperacetylated nucleosomes.

Role of Drug Structure in the Recognition of Nucleosomal DNA Targets. The observed differences between calicheamicin and an analog missing the terminal sugar and aromatic ring, esperamicin C, highlight the critical role played by the intact tetrasaccharide in calicheamicin target recognition. At the level of naked DNA, the two drugs differ significantly in the sequence-selectivity of DNA damage, as

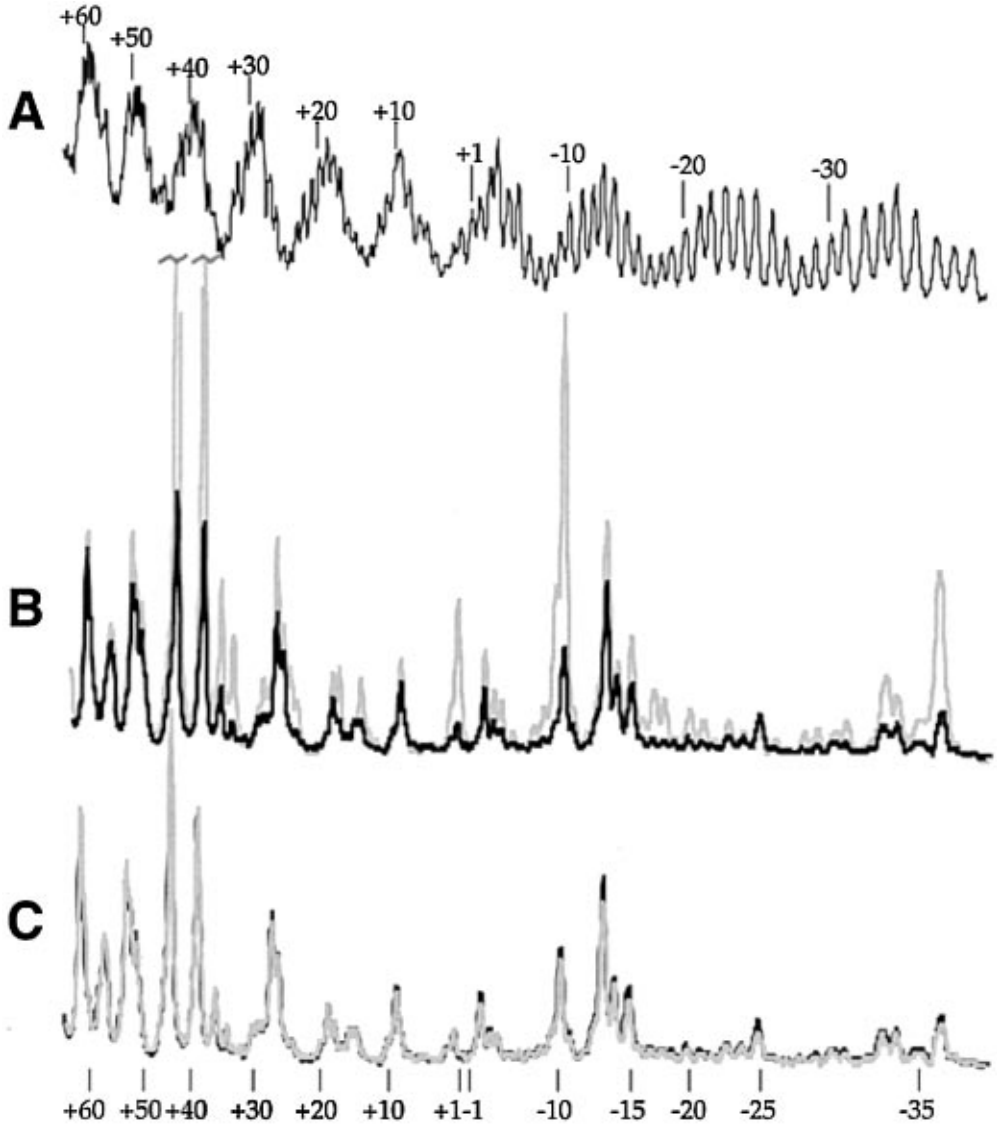

FIGURE 5: Cleavage profiles for esperamicin C and hydroxyl radical in normal and hyperacetylated nucleosomes. The gel shown in Figure 3 was subjected to phosphorimager analysis presented here as line graphs of damage frequency along the 5S rDNA sequence. (A) Hydroxyl radical cleavage of hyperacetylated nucleosomes; the pattern is identical to that produced in normal nucleosomes (data not shown). (B) Overlay of the damage patterns produced by esperamicin C in naked DNA (gray) and normal nucleosomes (black). (C) Overlay of the damage patterns produced by calicheamicin in normal (black) and hyperacetylated nucleosomes (gray). The sequence reads 5′ to 3′ from right to left, with numbering according to the position in the 5S rDNA construct.

shown in Figure 4B and 5B. Calicheamicin shows a preference for the 3′-ends of purine tracts (*2*, *4*) and to cause bending of the DNA upon binding (*21*), with the tetrasaccharide side chain responsible for this selectivity (A. A. Salzberg, and P. C. Dedon, unpublished observations). However, truncation of the side chain to produce esperamicin C results in a poorly definable sequence selectivity, except for a preference for pyrimidines and a lower affinity for DNA. The latter is apparent in the higher concentration (1.5 μM) of esperamicin C required to produce levels of DNA damage similar to calicheamicin (160 nM; Figure 3).

One of the most obvious differences between the two molecules is their sensitivity to the nucleosome-induced conformational changes in DNA at positions −13 and −14. Calicheamicin damage is enhanced severalfold at these sites in the 5S rDNA nucleosome compared to naked DNA (Figure 4B; *4*), possibly due to nucleosome-induced bending of the DNA (*21*). However, as shown in Figure 5B, this effect is not apparent with esperamicin C. The absence of enhanced DNA damage at positions −13 and −14 and the different sequence selectivity of esperamicin C points to the importance of the intact tetrasaccharide side chain in the targeting of purine tracts by calicheamicin and in drug-induced DNA bending.

ACKNOWLEDGMENT

The authors gratefully acknowledge the assistance of William LaMarr, Aaron Salzberg, Jinghai Xu, and other members of the Dedon lab for their guidance, stimulating discussions, and critical reading of the manuscript.

REFERENCES

1. Worpehoski, M. A., & Hurley, L. H. (1988) *Chem. Res. Toxicol. 1*, 315−333.
2. Kuduvalli, P. N., Townsend, C. A., & Tullius, T. D. (1995) *Biochemistry 34*, 3899−3906.
3. Yu, L., Goldberg, I. H., & Dedon, P. C. (1994) *J. Biol. Chem. 269*, 4144−4151.

4. Yu, L., Salzberg, A. A., & Dedon, P. C. (1995) *Bioorg. Med. Chem. 3*, 729−741.
5. Lee, M. D., Ellestad, G. A., & Borders, D. B. (1991) *Acc. Chem. Res. 24*, 235−243.
6. Dedon, P. C., & Goldberg, I. H. (1992) *Chem. Res. Toxicol. 5*, 311−332.
7. Dedon, P. C., Salzberg, A. A., & Xu, J. (1993) *Biochemistry 32*, 3617−3622.
8. Zein, N., Poncin, M., Nilakantan, R., & Ellestad, G. A. (1989) *Science 244*, 697−699.
9. Walker, S., Landovitz, R., Ding, W. D., Ellestad, G. E., & Kahne, D. (1992) *Proc. Natl. Acad. Sci. U.S.A. 89*, 4608−4612.
10. Zein, N., Ding, W.-D., & Ellestad, G. A. (1990) in *Molecular Basis of Specificity in Nucleic Acid-Drug Interactions* (Jortner, B. P. a. J., Ed.) pp 323−330, Kluwer Academic Publishers,
11. Mah, S. C., Price, M. A., Townsend, C. A., & Tullius, T. D. (1994) *Tetrahedron 50*, 1361−1378.
12. Walker, S., Murnick, J., & Kahne, D. J. (1993) *J. Am. Chem. Soc. 115*, 7954−7961.
13. Walker, S. L., Andreotti, A. H., & Kahne, D. E. (1994) *Tetrahedron 50*, 1351−1360.
14. Paloma, L. G., Smith, J. A., Chazin, W. J., & Nicolaou, K. C. (1994) *J. Am. Chem. Soc. 116*, 3697−3708.
15. Kumar, R. A., Ikemoto, N., & Patel, D. J. (1997) *J. Mol. Biol. 265*, 187−201.
16. Ikemoto, N., Kumar, R. A., Ling, T. T., Ellestad, G. A., Danishefsky, S. J., & Patel, D. J. (1995) *Proc. Natl. Acad. Sci. U.S.A. 92*, 10506−10510.
17. Aiyar, J., Danishefsky, S. J., & Crothers, D. M. (1992) *J. Am. Chem. Soc. 114*, 7552−7554.
18. Drak, J., Iwasawa, N., Danishefsky, S., & Crothers, D. M. (1991) *Proc. Natl. Acad. Sci. U.S.A. 88*, 7464−7468.
19. Nicolaou, K. C., Tsay, S.-C., Suzuki, T., & Joyce, G. F. (1992) *J. Am. Chem. Soc. 114*, 7555−7557.
20. Sugiura, Y., Uesawa, Y., Takahashi, Y., Kuwahara, J., Golik, J., & Doyle, T.W. (1989) *Proc. Natl. Acad. Sci. U.S.A. 86*, 7672−7676.
21. Salzberg, A., Mathur, P., & Dedon, P. (1996) in *DNA and RNA Cleavers and Chemotherapy of Cancer and Viral Diseases* (Meunier, B., Ed.) pp 23−36, Kluwer Academic Publishers, Dordrecht.
22. Krishnamurthy, G., Ding, W.-d., O'Brien, L., & Ellestad, G. A. (1994) *Tetrahedron 50*, 1341−1349.
23. Wolffe, A. (1992) *Chromatin Structure and Function*, Academic Press, San Diego.
24. van Holde, K. E. (1989) *Chromatin*, Springer-Verlag, New York.
25. Hayes, J. J., Tullius, T. D., & Wolffe, A. P. (1990) *Proc. Natl. Acad. Sci. U.S.A. 87*, 7405−7409.
26. Richmond, T. J., Finch, J. T., Rushton, B., Rhodes, D., & Klug, A. (1984) *Nature 311*, 532−537.
27. Hogan, M. E., Rooney, T. F., & Austin, R. H. (1987) *Nature 328*, 554−557.
28. Davie, J. R., & Hendzel, M. J. (1994) *J. Cell. Biochem. 55*, 98−105.
29. Loidl, P. (1994) *Chromosoma 103*, 441−449.
30. Bauer, W. R., Hayes, J. J., White, J. H., & Wolffe, A. P. (1994) *J. Mol. Biol. 236*, 685−690.
31. Oliva, R., Bazett-Jones, D. P., Locklear, L., & Dixon, G. H. (1990) *Nucleic Acids Res. 18*, 2739−2747.
32. Lee, D. Y., Hayes, J. J., Pruss, D., & Wolffe, A. P. (1993) *Cell 72*, 73−84.
33. Norton, V. G., Imai, B. S., Yau, P., & Bradbury, E. M. (1989) *Cell 57*, 449−457.
34. Bode, J., Gómez-Lira, M. M., & Schröter, H. (1983) *Eur. J. Biochem. 130*, 437−445.
35. Ausio, J., & van Holde, K. E. (1986) *Biochemistry 25*, 1421−1428.
36. Yu, L., Golik, J., Harrison, R., & Dedon, P. (1994) *J. Am. Chem. Soc. 116*, 9733−9738.
37. Wolffe, A. P., Jordan, E., & Brown, D. D. (1986) *Cell 44*, 381−389.
38. Riggs, M. G., Whittaker, R. G., Neumann, J. R., & V. M., I. (1978) *Cold Spring Harb. Symp. Quant. Biol. 42 (2)*, 815−818.
39. Vidali, G., Boffa, L. C., Bradbury, E. M., & Allfrey, V. G. (1978) *Proc. Natl. Acad. Sci. U.S.A. 75*, 2239−2243.
40. Simon, R. H., & Felsenfeld, G. (1979) *Nucleic Acids Res. 6*, 689−696.
41. Wolffe, A. P. (1988) *EMBO J. 7*, 1071−1079.
42. Price, M. A., & Tullius, T. D. (1992) *Methods Enzymol. 212*, 194−218.
43. Maxam, A., & Gilbert, W. (1980) *Methods Enzymol. 65*, 499−560.
44. Zein, N., Sinha, A. M., McGahren, W. J., & Ellestad, G. A. (1988) *Science 240*, 1198−1201.
45. Chatterjee, M., Mah, S. C., Tullius, T. D., & Townsend, C. A. (1995) *J. Am. Chem. Soc. 117*, 8074−8082.

BI9718393